ACCOUNTS
of chemical research

Control of Charge Transfer in Donor/Acceptor Metal−Organic Frameworks

HITOSHI MIYASAKA*

Department of Chemistry, Division of Material Sciences, Graduate School of Natural Science and Technology, Kanazawa University, Kakuma-machi, Kanazawa 920-1192, Japan

RECEIVED ON APRIL 5, 2012

CONSPECTUS

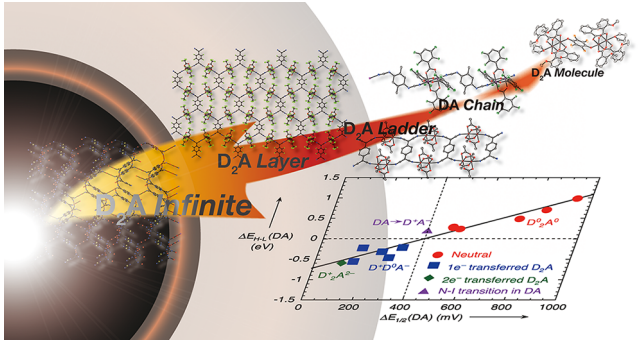

Charge transfer (CT) of $D^0A^0 \leftrightarrow D^{\delta+}A^{\delta-}$ not only involves an electron transfer from D to A, but also generates a new spin set of $S = 1/2$ spins with an exchange interaction. Therefore, the control of CT in multidimensional frameworks could be an efficient way to design electronically/magnetically functional materials. The use of redox-active metal complexes as D and/or A building blocks expands the variety of such D/A frameworks with the formulation of D_mA_n (m, $n \geq 1$), permitting the design of donor/acceptor metal−organic frameworks (D/A-MOFs). This Account summarizes our ongoing research on the design of D/A-MOFs and on the systematic control of CT in such D/A-MOFs toward the discovery of unique electronic/magnetic materials exhibiting nontrivial phenomena. For this purpose, the D/A combinations of carboxylate-bridged paddlewheel-type diruthenium(II,II) complexes ($[Ru_2^{II,II}]$) that act as one-electron ($1e^-$) donors and polycyanoorganic acceptors such as 7,7,8,8-tetracyano-*p*-quinodimethane (TCNQ) and *N*,*N*′-dicyanoquinodiimine (DCNQI) have been chosen.

Even in the covalently bonded motif, the CT in this system is systematically dependent on the intrinsic ionization potential (I_D) and electron affinity (E_A) of the D and A units, respectively, which is controllable by chemical modification of the D/A units. As we consider the energy difference between the HOMO of D and the LUMO of A ($\Delta E_{H\text{-}L}(DA)$) instead of $h\nu_{CT} \propto |I_D - E_A|$, the neutral (N) and ionic (I) states can be defined as follows: (i) the D/A materials with $\Delta E_{H\text{-}L}(DA) > 0$ (i.e., the LUMO level of A is higher than the HOMO level of D) should be neutral, and (ii) complexes adopted when $\Delta E_{H\text{-}L}(DA) < 0$ are, meanwhile, ionic. Materials located near $\Delta E_{H\text{-}L}(DA) \approx 0$, that is, at the boundary between the N and I phases, are candidates for the N−I transition driven by external stimuli such as temperature, pressure, and photoirradiation. Even in the ionic state, two distinct states could be isolated for the D_2A type: (ii-1) the $1e^-$ transferred D_2A-MOFs provide mixed-valence systems of $D^+D^0A^-$ possibly involving intervalence CT, which produce magnetic correlations via radical A^- units, and (ii-2) when the $2e^-$ reduced form of A (e.g., $TCNQ^{2-}$) is energetically favored beyond the on-site Coulomb repulsion on A, the oxidation state of $D^+{}_2A^{2-}$ is produced, for which magnetic measurements reveal a paramagnetic state attributed to the isolated D^+ units.

The interspatial Coulombic interaction is another factor in determining the charge distribution in materials, which is related to the spatial Coulombic stability of D/A packing and possibly yields a mixture of N and I domains when it is more advantageous to get Coulombic gain than in the uniform N or I phase. Such a phase could be observed at the boundary between N and I phases involving the N−I transition.

These charge-distributed states/phases are systematically demonstrated in a D/A-MOF system made by the combination of $[Ru_2^{II,II}]$ and TCNQ/DCNQI; however, we immediately recognize the charge distribution of D/A-MOF only by understanding the nature of the starting D/A units. The present D/A-MOF system should be an intriguing platform to look for new functionalities with synergistic correlations among charge, spin, and lattice.

Published on the Web 11/05/2012 www.pubs.acs.org/accounts
10.1021/ar300102t

Introduction

The charge transfer (CT) of $D^0A^0 \leftrightarrow D^{\delta+}A^{\delta-}$, involving an electron transfer from donor (D) to acceptor (A), possibly generates charge distributions, a new spin set of generated $S = 1/2$ spins with an exchange interaction, and a structural modification in the ionic form of $D^{\delta+}A^{\delta-}$. These changes directly link to typical physical properties of electron/hole transports, magnetic ordering, and dielectric responses at the bulk level. Consequently, we realized that the design of CT systems is an efficient way to discover novel functional materials such as magnetic/conductive synergistic (or hybrid) materials.[1−3] Nevertheless, most D/A assembled systems have only been established in D/A supramolecular assemblies based on organic molecules in a π-stacking motif,[4] which unfortunately cannot derive multiple spin states except for a triplet state caused by a ferromagnetic coupling of generated $S = 1/2$ spins.[5]

Important advantages of the use of metal complexes as D and/or A are: (i) a large variety of redox-active metal complexes are candidates, compared with organic molecules; (ii) the coordination bonding can be used to connect *directly* between D and A; (iii) most of them are stereospecific, and the topology of the coordinating sites defines the lattice dimension when they are assembled to construct metal−organic frameworks of D/A (called D/A-MOFs); (iv) the static multiple spin state on d-orbitals can be used in addition to transferring electrons; and (v) various types of CT such as metal-to-metal, metal-to-ligand, ligand-to-metal, and ligand-to-ligand CTs associated with d- and p-orbital electrons are available. Actually, however, it is not easy to choose a good D/A set, because we must tune the ionization potential (I_D) of D and the electron affinity (E_A) of A to control the CT in addition to the design of a purposeful molecular system.

Now, we consider one-electron ($1e^-$) transfer from D to A (Figure 1), namely, D and A only have the potential to permit $1e^-$ transfer. As a 1:1 assembly is assumed, this DA system is only able to produce CT from $D^0A^0 \leftrightarrow D^{\delta+}A^{\delta-}$ involving a neutral (N)−ionic (I) transition, which is basically tuned by the relation between I_D and E_A of D and A, respectively. Thus, as the degree of CT (δ) is not partial as $\delta < 1$, the DA system can take only two limited states of N and I, and this fact should also be adopted in the expanded one-dimensional (*1-D*) system of $(DA)_n$ (the dimensionality of the lattice, *1-D*, *2-D*, and *3-D*, is hereafter written in italic form to distinguish it from "D" as donor). Meanwhile, as a D/A = 2:1 assembly is taken, this D_2A system also involves the N−I transition to produce the $D^0D^+A^-$ state. An important point is that such

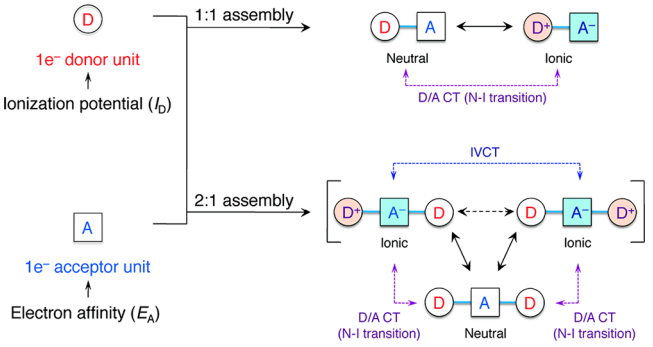

FIGURE 1. Proposed schemes of CT in DA and D_2A systems, where the DA system only shows an N−I transition, whereas the D_2A system involves the N−I transition followed by IVCT between degenerate ionic states.

an I state is not static, but has a resonance of $[D^0D^+A^- \leftrightarrow D^+D^0A^-]$ with mixed-valence states such as the Creutz−Taube ion,[6] if the N−I transition preliminarily occurred without any structural modification, where the HOMO levels in a double-minimum potential are half-occupied on average with one electron involving intervalence CT (IVCT) dependent on the resonance gap.[7] The expansion of D_2A to *2-D* and *3-D* networks possibly produces a set of a half-occupied bonding band and an unoccupied antibonding band with a Fermi level at the 1/4 range of the bonding band, even if the feature of the band is strongly dependent on the structure and packing of materials.[3,4] This is an essential synthetic strategy for molecular conducting materials with D_nA.

In the development of molecular functional materials, research on CT materials based on transition metal complexes is still less advanced, despite the CT materials being a "reservoir of functions". This would be, simply, because several factors must be controlled at once. However, I believe that the use of redox-active metal complexes as D and/or A broadens our perspective on the design of systems, and a systematic investigation would bring us close to the goal. Our goal is to achieve the systematic control of CT in D/A-MOFs and rationally to obtain unique electronic/magnetic materials exhibiting nontrivial phenomena. This Account summarizes our ongoing research on the design of D/A-MOFs and on the systematic control of CT in such materials.

Choice of Building Blocks as D and A

Following the aforementioned strategy, we have chosen a family of carboxylate-bridged paddlewheel-type diruthenium(II,II) complexes (abbreviated henceforth as $[Ru_2^{II,II}]$, see Figure 2a) and organic polycyano molecules such as 7,7,8,8-tetracyano-*p*-quinodimethane (TCNQ) and *N*,*N*′-dicyanoquinodiimine (DCNQI) (see Figure 2a) as D and A, respectively. The paddlewheel-type dimetal modules not

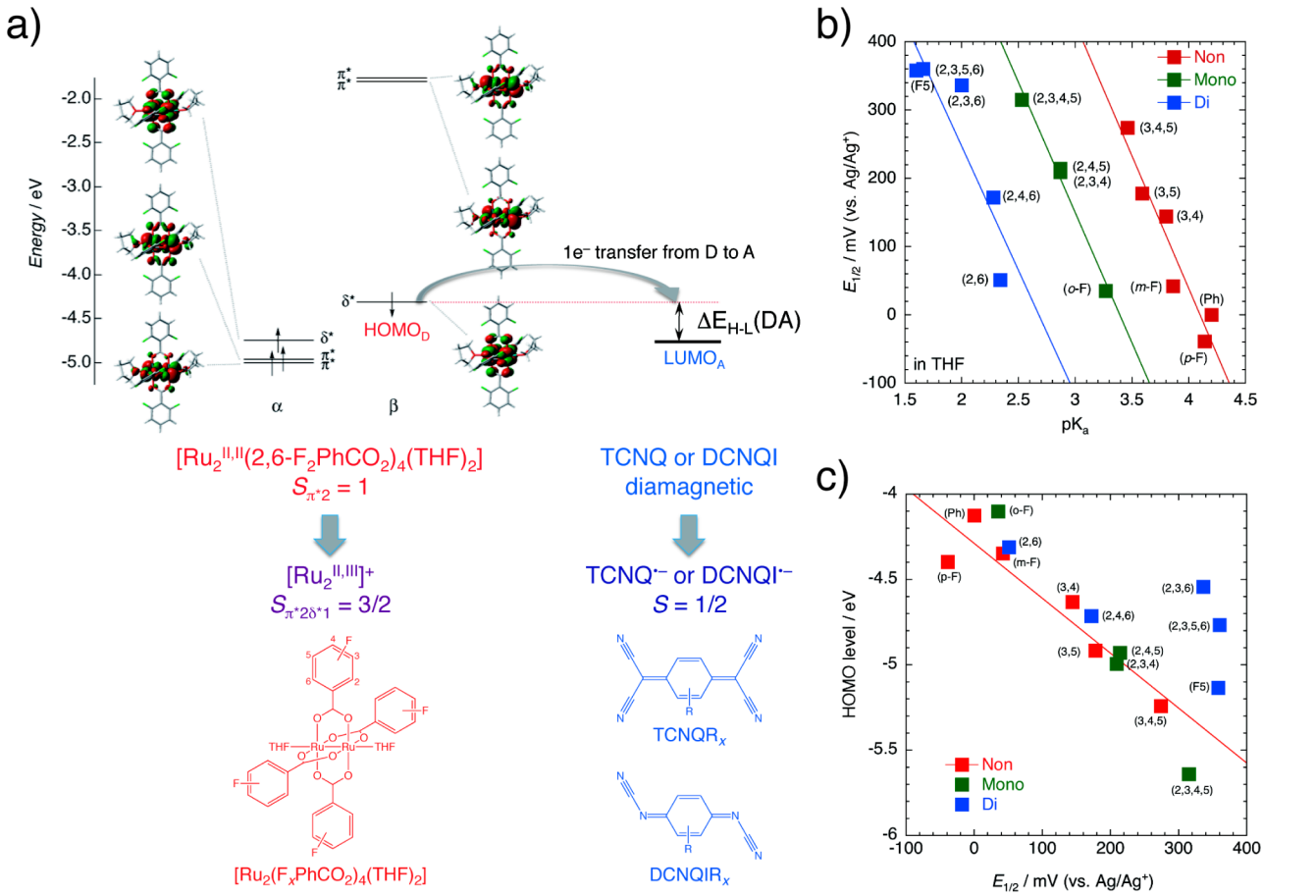

FIGURE 2. Relation between the HOMO energy level and redox properties in the family of F-substituted benzoate-bridged $[Ru_2^{II,II}]$ complexes, $[Ru_2^{II,II}(F_xPhCO_2)_4(THF)_2]$. (a) Frontier orbitals associated with the π^* and δ^* orbitals of $[Ru_2^{II,II}(2,6\text{-}F_2PhCO_2)_4(THF)_2]$ and their energy levels (eV), where δ^* for the β electron corresponds to the $HOMO_D$ level and the β electron transfers to $LUMO_A$ of acceptors. (b) Plot of half-wave redox potential ($E_{1/2}$) vs pK_a of the corresponding benzoic acids, where $E_{1/2}$ are values measured in THF with a Ag/Ag^+ reference electrode. The red, green, and blue solid lines represent the linear least-squares fitted lines for non-, mono-, and di-*o*-F substituted groups, respectively. (c) Plot of HOMO ($\delta^*(\beta)$) level vs $E_{1/2}$, where the solid red line represents the least-squares linear line for the non-*o*-F group. Energy levels were calculated based on DFT with the UB3LYP method using LANL2TZ(f) basis functions for Ru and LANL2DZpd basis functions for the other atoms. Parts (b) and (c) reproduced with permission from ref 15. Copyright 2011 The Royal Society of Chemistry.

only, in structural terms, act as a building block as a node or edge for the frameworks,[8] but also, in intrinsic properties, function as a spin source, redox-active module, and reaction site for catalysts.[9−11] Indeed, the $[Ru_2^{II,II}]$ unit, acting as a linear coordinating-acceptor with axial labile sites to form an "edge" in frameworks (Figure 3),[12,13] has the high redox-activity to derive $[Ru_2^{II,III}]^+$ without significant structural change. This fact, the structure being basically independent of its charge, is favorable for electron transport; conversely, the structural transition tends to promote charge localization as a Peierls transition. It should also be noted that both species of $[Ru_2^{II,II}]$ and $[Ru_2^{II,III}]^+$ are paramagnetic with $S = 1$ and $S = 3/2$, respectively, available as a magnetic source with multiple spin states in both oxidation states.[14]

Another important factor in choosing the family of $[Ru_2^{II,II}]$ as D against TCNQ or DCNQI is that its HOMO level ($HOMO_D$) is widely tunable by modifying the carboxylate bridges to locate its HOMO level near the LUMO level ($LUMO_A$) of TCNQ/DCNQI derivatives (Figure 2). In particular, this fact indicates that it is possible to tune the gap ($\Delta E_{H\text{-}L}(DA)$) between $HOMO_D$ and $LUMO_A$ by chemical modification of the carboxylate ligands on $[Ru_2^{II,II}]$ and the R-substituents on $TCNQR_x$/$DCNQIR_x$. Figure 2a shows HOMO and SOMO (= Single Occupied Molecular Orbital) frontier orbitals with the energy level of $[Ru_2^{II,II}(2,6\text{-}F_2PhCO_2)_4(THF)_2]$ ($2,6\text{-}F_2PhCO_2^-$ = 2,6-difluorobenzoate) calculated based on density functional theory (DFT).[15] The $HOMO_D$ and $SOMO_D$ correspond to δ^* and π^* orbitals of the Ru−Ru bond, respectively, and the β spin of δ^* is removed in the oxidation by acceptors.[9] Taking an example of the family of $[Ru_2^{II,II}]$ complexes bearing fluorine-substituted benzoate equatorial ligands ($[Ru_2^{II,II}(F_xPhCO_2)_4(THF)_2]$), the first redox potential ($^1E_{1/2}$ vs Ag/Ag^+ in THF) varies

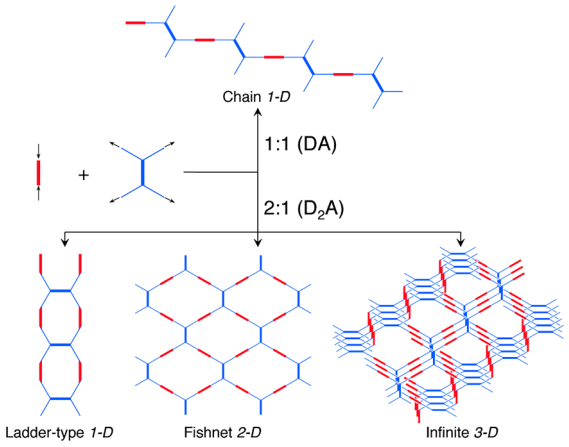

FIGURE 3. Possible metal−organic frameworks (MOFs) constructed by assembly of $[Ru_2^{II,II}]$ (red unit) and TCNQ (blue unit) in a 1:1 or 2:1 ratio, regarded as D/A-MOFs.

in the wide range between −50 and +400 mV (Figure 2b). This variation is directly associated with the $HOMO_D$ level ($\delta^*(\beta)$) in the energy range of −4.4 to −5.7 eV (Figure 2c).[15]

In contrast, TCNQ and DCNQI and their derivatives are well-known organic electron acceptors, which experience two-step reductions as follows: $A + e^- \rightarrow A^{\bullet -}$ (first) and $A^{\bullet -} + e^- \rightarrow A^{2-}$ (second). Because the radical anion species ($A^{\bullet -}$), however, are relatively stable because the potential difference between $^1E_{1/2}$ and $^2E_{1/2}$ (noted as $|^2E_{1/2} - {}^1E_{1/2}|$) is relatively wide at 500−600 mV for $TCNQR_x$ and $DCNQIR_x$, this type of acceptor is often treated as a $1e^-$ acceptor depending on the donors used.[4] It goes without saying that substitution on $TCNQR_x$/$DCNQIR_x$ varies the electrochemical potential, and concomitantly, the $LUMO_A$ level with E_A tunes $\Delta E_{H\text{-}L}(DA)$.

TCNQ and its derivatives ($TCNQR_x$) act as tetradentate coordinating-donor building blocks, which enable the creation of various types of frameworks,[16] such as linear-type *1-D* chains, ladder-type *1-D* chains,[17] fishnet-type *2-D* networks, and infinite *3-D* networks, by assembling with linear-type coordinating-acceptor building blocks as $[Ru_2]$ complexes (Figure 3). DCNQI and its derivatives ($DCNQIR_x$), which act as bidentate coordinating-donor building blocks,[18,19] can form *1-D* chains assembling with $[Ru_2]$.

Validation of Varying Ionicity Depending on Acceptors

The reaction of $[Ru_2^{II,II}(CF_3CO_2)_4(THF)_2]$ with TCNQ leads to the formation of a *2-D* fishnet-type network composed of a 2:1 ratio of $[Ru_2^{II,II}]$/TCNQ (Figure 3): $[\{Ru_2(CF_3CO_2)_4\}_2TCNQ]\cdot 3$(toluene). Indeed, this material, which is the first example of the family of $[Ru_2^{II,II}]$/TCNQ D/A−MOFs, fortunately had a highly symmetrical structure with only one structurally independent $[Ru_2]$ unit even for the D_2A type.[20] At first, we wished to follow the scheme for ionic D_2A in Figure 1, which includes electron transfer of $[Ru_2^{II,II}] \rightarrow$ TCNQ followed by IVCT associated with $[Ru_2^{II,II}]$ and $[Ru_2^{II,III}]^+$ species; unfortunately, the material was neutral without virtual charge separation. The neutral form can be easily confirmed by measuring the magnetic property of the material, which leads to the paramagnetic nature of $[Ru_2^{II,II}]$ with $S = 1$ strongly affected by anisotropy with $D_{S=1} \approx 250-300$ cm^{-1}.[9] Therefore, the acceptor was changed from TCNQ to $TCNQF_4$, which has a much larger E_A than that of TCNQ. As expected, the isostructural material, $[\{Ru_2(CF_3CO_2)_4\}_2TCNQF_4]\cdot 3$(toluene), showed a virtual CT to induce the formal state $[\{Ru_2\}^{0.5+}-(TCNQF_4^{\bullet -})-\{Ru_2\}^{0.5+}]$ with IVCT.[21,22] Similarly, the $TCNQR_x$ unit of $[\{Ru_2(CF_3CO_2)_4\}_2TCNQR_x]$ was varied in the series $TCNQF_2$, $TCNQCl_2$, $TCNQBr_2$, $TCNQMe_2$, and $TCNQ(MeO)_2$, in addition to TCNQ and $TCNQF_4$. However, all materials, except for $TCNQF_4$, are virtually neutral.[23]

Rather than CT complexes based on metal complexes, organic CT complexes have been an important target in the design of functional materials to date: We can learn a lot from these good examples; for example, the ionicity of appropriate series of D/A sets has often been investigated. A representative example is Torrance's V-shaped diagram displaying CT transition energies ($h\nu_{CT}$) vs the difference in first-redox potentials between D and A ($\Delta E_{1/2}(DA) = {}^1E_{1/2}(D) - {}^1E_{1/2}(A)$) for several π-stacked organic CT complexes, which reveals a scaling relation to separate the N and I forms.[24] This relationship has been widely applicable in such series as π-stacked organic D/A systems,[4] and specific materials exhibiting temperature-induced N−I transitions have successfully been found in the vicinity of the valley of the V-shape.[24] This type of diagram should have the ability to be expanded to metal-complexes D/A systems. Unfortunately, however, it is difficult to apply to such systems as our D/A-MOF system exhibiting wide absorptions at low energies such as the $\pi-\pi^*$ transition on TCNQ, IVCT, and CT bands related to conducting together with $h\nu_{CT}$ for D ↔ A, because of the difficulty in accurately assigning individual transitions. Therefore, the energy gap ($\Delta E_{H\text{-}L}(DA)$, see Figure 2) between the $HOMO_D$ level of $[Ru_2^{II,II}(CF_3CO_2)_4(THF)_2]$ and the $LUMO^A$ level of $TCNQR_x$ was used instead of $h\nu_{CT}$, where the $HOMO_D$ and $LUMO_A$ levels of units were determined by DFT calculations using the atomic coordinates determined from single-crystal X-ray crystallography for $[Ru_2^{II,II}(CF_3CO_2)_4(THF)_2]$[25] and computer-optimized for $TCNQR_x$. Figure 4a shows the plot of $\Delta E_{H\text{-}L}(DA)$ vs $\Delta E_{1/2}(DA)$ in the

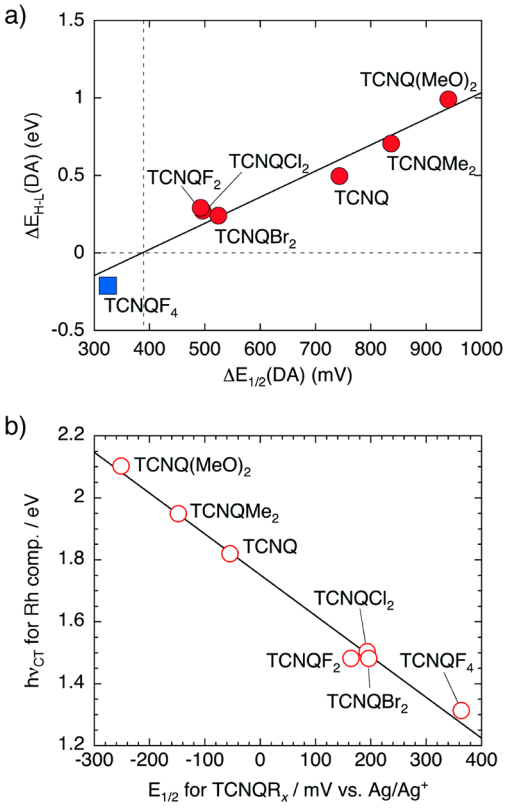

FIGURE 4. Plots of the energy gap between the HOMO level of $[Ru_2^{II,II}(CF_3CO_2)_4(THF)_2]$ and the LUMO level of $TCNQR_x$ estimated by DFT calculations ($\Delta E_{H\text{-}L}$(DA)) vs $\Delta E_{1/2}$(DA) (a) and the CT energies of $[\{Rh_2^{II,II}(CF_3CO_2)_4\}_2TCNQR_x]$ ($h\nu_{CT}$ of Rh comp.) vs $E_{1/2}(TCNQR_x)$ (b). Reproduced with permission from ref 23. Copyright 2012 The Royal Society of Chemistry.

family of $[\{Ru_2(CF_3CO_2)_4\}_2TCNQR_x]$.[23] There is a linear trend in this plot, and only $[\{Ru_2(CF_3CO_2)_4\}_2TCNQF_4]$ has a negative value of $\Delta E_{H\text{-}L}$(DA) with the smallest $\Delta E_{1/2}$(DA) of ≈325 mV. The crossover point of the least-squares linear fitted line with $\Delta E_{H\text{-}L}$(DA) = 0 is ≈390 mV, suggesting a boundary between N and 1e$^-$ transferred I forms, that is, corresponding to the Madelung energy of this system; $M = I_D - E_A$.[26] Limiting to this family, this variation is attributed to the nature of $TCNQR_x$. In fact, this trend can be seen in the plot of $h\nu_{CT}$ experimentally obtained for the isostructural family of $[\{Rh_2^{II,II}(CF_3CO_2)_4\}_2TCNQR_x]$ as a function of $^1E_{1/2}(TCNQR_x)$ (Figure 4b).[23] Thus, only $[\{Ru_2(CF_3CO_2)_4\}_2TCNQF_4]$ with a negative value of $E_{H\text{-}L}$(DA) is able to produce charge separation, and this presumption is in complete agreement with the experimental observation.[21,22]

An Ionicity Diagram for Systematic Investigation of CT in the $[Ru_2^{II,II}]$/TCNQ, DCNQI System

The ionicity diagram made by the plot of $\Delta E_{H\text{-}L}$(DA) vs $\Delta E_{1/2}$(DA) could be basically extended to all of the D/A family

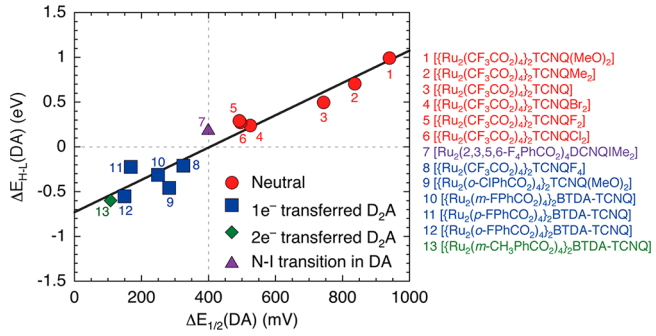

FIGURE 5. Plot of $\Delta E_{H\text{-}L}$(DA) vs $\Delta E_{1/2}$(DA) for D_2A and DA materials of $[Ru_2^{II,II}]$/$TCNQR_x$, $DCNQIR_x$ sets reported up until now (2,3,5,6-$F_4PhCO_2^-$ = 2,3,5,6-tetrafluorobenzoate; *o*-$ClPhCO_2^-$ = *o*-chlorobenzoate; *x*-$FPhCO_2^-$ = *x*-fluorobenzoate with *x*- = *o*-, *m*-, *p*-; *m*-$CH_3PhCO_2^-$ = *m*-methylbenzoate).

synthesized by the reaction of $[Ru_2^{II,II}(R'CO_2)_4(THF)_2]$ and $TCNQR_x$ or $DCNQIR_x$, because the validity of this ionicity diagram is essentially only dependent on the accuracy of the DFT calculations. $\Delta E_{H\text{-}L}$(DA) was plotted as a function of $\Delta E_{1/2}$(DA) for the 13 materials reported up until now, as shown in Figure 5. The linear relation is certainly adopted in the expanded family even with a variety of D/A combinations. The crossover point of the least-squares linear fitted line with $\Delta E_{H\text{-}L}$(DA) = 0 is ≈400 mV, consistent with only the case of $[\{Ru_2(CF_3CO_2)_4\}_2TCNQR_x]$ (Figure 4a). As explained above, the D/A combinations in the lower left space with $\Delta E_{H\text{-}L}$(DA) < 0 (blue and green squares in Figure 5) should be ionic, whereas those in the upper right space with $\Delta E_{H\text{-}L}$(DA) > 0 (red circle in Figure 5) are neutral. The actual charge distribution of all compounds is in good agreement with this classification. Very interestingly, a compound exhibiting an N−I transition was found just in a combination at the N−I boundary (purple triangle in Figure 5); this fact justifies the use of this ionicity diagram for the D/A family made from $[Ru_2^{II,II}(R'CO_2)_4(THF)_2]$ and $TCNQR_x$/$DCNQIR_x$.

1e$^-$ Transferred D_2A as Magnets

Compounds made from the D/A combinations located in the lower left square of Figure 5 with $\Delta E_{H\text{-}L}$(DA) < 0 could be ionic. However, if the $\Delta E_{H\text{-}L}$(DA) gap is very large in the D_2A system and overwhelms the on-site Coulomb repulsion on A, it may be possible to have a 2e$^-$ transferred D_2A, as mentioned in the next section; other ionic D_2A forms result from 1e$^-$ transferred D_2A. The 1e$^-$ transferred D_2A materials, with the formula $[\{Ru_2(R'CO_2)_4\}_2TCNQR_x]$ are very likely to be magnets because spins of $S = 3/2$ for $[Ru_2^{II,III}]^+$ and $S = 1$ for $[Ru_2^{II,II}]$ are aligned via $TCNQR_x^{\bullet-}$ with $S = 1/2$ through superexchange coupling spreading over the layer followed

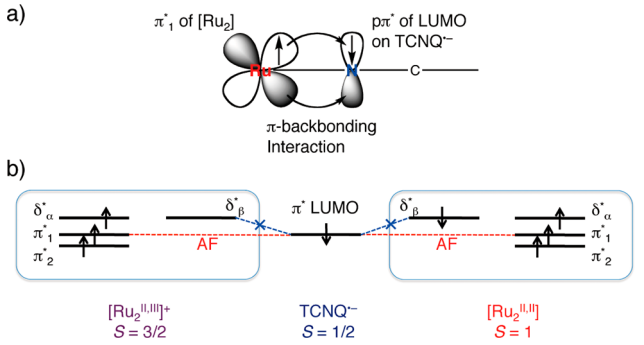

FIGURE 6. Schematic representations of orbital arrangements (a) and spin arrangements (b) between $[Ru_2]$ and $TCNQ^{\bullet-}$/$DCNQI^{\bullet-}$, where $LUMO_A$ of $TCNQ^{\bullet-}$/$DCNQI^{\bullet-}$ having a π-character strongly interacts with one of the π^* orbitals of $[Ru_2]$ (see Figure 2a) with the help of a π-back-donation mechanism, deriving an antiferromagnetic (AF) coupling, whereas the $LUMO_A$ of $TCNQ^{\bullet-}$/$DCNQI^{\bullet-}$ is not expected to show a strong magnetic coupling with the δ^* orbital of $[Ru_2]$.

by dipole−dipole interactions between layers to become finally a *3-D* magnet. It is noteworthy that the exchange coupling between $[Ru_2^{II,III}]^+$/$[Ru_2^{II,II}]$ and $TCNQR_x^{\bullet-}$ is expected to be very large for the following two reasons: (i) two spins of $[Ru_2^{II,III}]^+$/$[Ru_2^{II,II}]$ are in the π^* orbitals of the Ru−Ru bond, which can strongly couple antiferromagnetically with the SOMO with π-character of $TCNQ^{\bullet-}$, that is, as a result of Pauli's rule (Figure 6), and (ii) the energy levels of these orbitals are similar. Consequently, the spins of $[Ru_2^{II,III}]^+$/$[Ru_2^{II,II}]$ and $TCNQR_x^{\bullet-}$ are expected to order in a layer with a ferrimagnetic arrangement. However, this spin arrangement was not experimentally observed until recently because the strong magnetic correlation and anisotropy arising from $[Ru_2^{II,III}]^+$/$[Ru_2^{II,II}]$ made it difficult to distinguish either the ferro- or ferrimagnetic spin arrangement. Very recently, a *1-D* chain DA compound exhibiting an N−I transition has revealed the ferrimagnetic spin arrangement of $S = 3/2$ for $[Ru_2^{II,III}]^+$ and $S = 1/2$ for $DCNQI^{\bullet-}$ with the exchange coupling constant $J \approx -170$ K (anisotropy was not taken into account) in the I phase with a $[-D^+-A^--]$ motif.[27] In addition, it has been reported by Rey et al. that the exchange between $[Ru_2^{II,II}]$ and the organic radical is greater than −200 K.[28]

The interlayer interaction is very strong in this system on the whole, leading to the formation of *3-D* magnetic ordering at a relatively high temperature. $[\{Ru_2(CF_3CO_2)_4\}_2TCNQF_4]\cdot$ 3(toluene) shows antiferromagnetic order at $T_N = 95$ K.[21,22] It should be noted that this is not a simple antiferromagnet, but a field-induced ferrimagnet with a remnant magnetization of ≈36% and a large coercivity with $H_c \approx 2.32$ T. This interesting behavior should be due to the strong anisotropic nature of $[Ru_2^{II,II}]$ ($D_{S=1} \approx 250-300$ cm^{-1}) and $[Ru_2^{II,III}]^+$ ($D_{S=3/2} \approx 60-70$ cm^{-1}),[9,29] even if they have facial anisotropy, and low structural dimensionality as *2-D* layered materials. Indeed, this situation also causes a spin-canting state reflecting the interlayer environment associated with the symmetry between layers, the location of interstitial solvents, disorder of structures, structural defects, and so on. $[\{Ru_2(o\text{-}FPhCO_2)_4\}_2BTDA\text{-}TCNQ]$ (BTDA-TCNQ = bis[1,2,5]-thiadizolotetracyanoquinodimethane) shows antiferromagnetic order at $T_N = 93$ K followed by a spin-canting order at $T_{c1} = 87$ K and a rearrangement at $T_{c2} = 13$ K,[30] whereas $[\{Ru_2(p\text{-}FPhCO_2)_4\}_2BTDA\text{-}TCNQ]$ shows a *3-D* ferrimagnet order at $T_c = 83$ K. Thus, the interlayer environment in the layered D_2A compounds is crucial in deciding the state of the magnets. An intriguing example is $[\{Ru_2(o\text{-}ClPhCO_2)_4\}_2TCNQ\text{-}(MeO)_2]\cdot CH_2Cl_2$, which reversibly changes its magnetic behavior between antiferromagnet with $T_N =$ 75 K and ferrimagnet with $T_c = 56$ K by solvation/desolvation of CH_2Cl_2 located between the layers, although the only discernible difference is ordering/disordering of a pendant ligand orientation without crucial change of the layer's lattice in the solvation/desolvation process.[31]

The D_2A type can also form a *3-D* lattice (Figure 3), in which the magnetism is only dependent on the exchange coupling through the lattice. While $[\{Ru_2(x\text{-}FPhCO_2)_4\}_2$-BTDA-TCNQ] with *x-* = *ortho-* and *para-* have the aforementioned *2-D* lattices,[30] the compound with *x-* = *meta-* has a *3-D* lattice in the same D_2A type.[32] Consequently, this *3-D* material simply produces a ferrimagnetic order at $T_c = 107$ K. This T_c, interestingly, decreases with increasing pressure.[33] This means that rather than the effect on the bond distance, the effect of pressure on the bond angle of Ru−N−C is crucial in this compound, probably reducing the overlap integral for the superexchange.

2e$^-$ Transferred D_2A with the Diamagnetic $TCNQ^{2-}$

Choosing an adequate combination of $[Ru_2^{II,II}]$ and $TCNQR_x$, the 2e$^-$ transferred state in the D_2A system with a formal state of $[\{Ru_2^{II,III}\}^+-(TCNQR_x^{2-})-\{Ru_2^{II,III}\}^+]$ can be isolated. However, in this case, the $\Delta E_{H\text{-}L}$(DA) must be very large to overcome the on-site Coulomb repulsion on $TCNQR_x^{2-}$; $|^2E_{1/2}(A) - {}^1E_{1/2}(A)| = 500-600$ mV for $TCNQR_x$. The combination of $[Ru_2^{II,II}(m\text{-}MePhCO_2)_4]$ (*m*-$MePhCO_2^-$ = *m*-methylbenzoate) and BTDA-TCNQ led to the formation of 2e$^-$ transferred D_2A in a *3-D* infinite network.[34] The important aspect is that this D/A combination has the largest negative $\Delta E_{H\text{-}L}$(DA) (≈ −0.6 eV) and the smallest $\Delta E_{1/2}$(DA) (≈ 110 mV) among the 13 materials in Figure 5. Figure 5 was modified into a plot as a

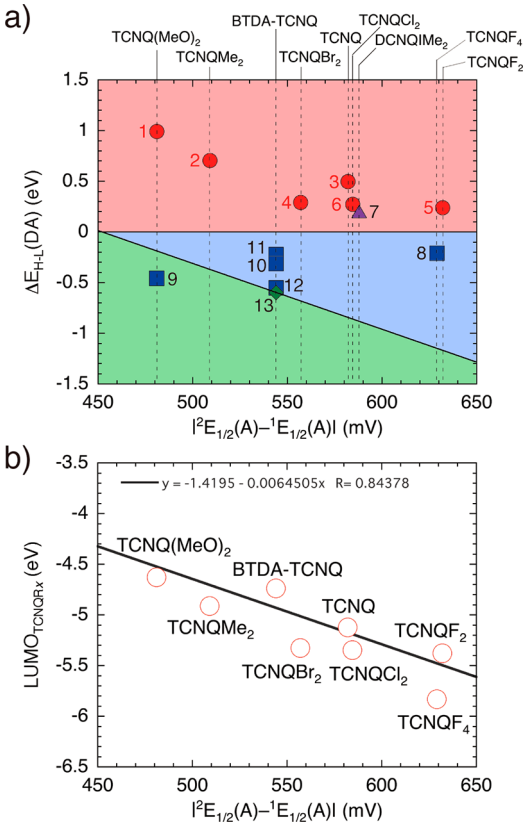

FIGURE 7. Plots of $\Delta E_{H\text{-}L}$(DA) (a) and $LUMO_A$ (b) vs $|^2E_{1/2}(A) - {}^1E_{1/2}(A)|$, where the least-squares fitted line obtained in the (b) plot was added to the (a) plot based on [{$Ru_2^{II,III}$(*m*-$MePhCO_2$)$_4$}$_2$(BTDA-TCNQ)] (No. 13).[34]

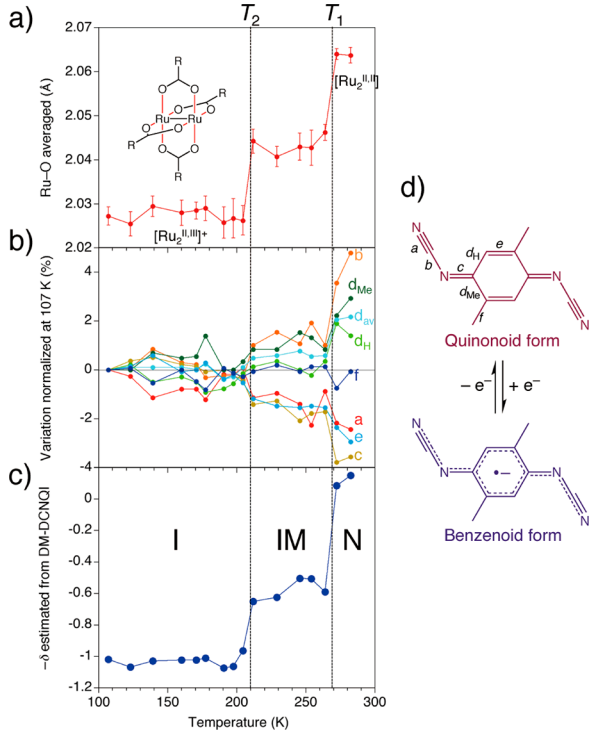

FIGURE 8. Variation of averaged Ru–O_{eq} bond length (a), respective bonds of the DMDCNQI unit (b), and the charge δ estimated from the DMDCNQI unit (c) as a function of temperature, where the structure was determined in the monoclinic space group $P2_1/n$ in the entire temperature range, and a schematic representation of the structure of DMDCNQI (d). Parts (a), (b), and (c) adapted with permission from ref 27. Copyright 2011 American Chemical Society.

function of $|^2E_{1/2}(A) - {}^1E_{1/2}(A)|$ (Figure 7a), in which the on-site Coulomb repulsion of the respective $TCNQR_x$ units is different, and we noticed that $TCNQ(MeO)_2$ is the smallest among the compounds. The plot of the $LUMO_A$ level vs $|^2E_{1/2}(A) - {}^1E_{1/2}(A)|$ roughly shows a linear relation (Figure 7b), and then the least-squares line was inserted into Figure 7a only fixing the slope based on the value of [{$Ru_2^{II,III}$(*m*-$MePhCO_2$)$_4$}$_2$(BTDA-TCNQ)]. Thus, we suppose that materials having lower $\Delta E_{H\text{-}L}$(DA) values than the inserted line are candidates for the $2e^-$ transferred system (green region in Figure 7a). Finally, a note about its magnetic properties: because $TCNQR_x^{2-}$ is diamagnetic, [{$Ru_2^{II,III}$(*m*-$MePhCO_2$)$_4$}$_2$(BTDA-TCNQ)] shows an isolated paramagnetic behavior with $S = 3/2$ arising from two [$Ru_2^{II,III}$(*m*-$MePhCO_2$)$_4$]$^+$ units.[34]

N–I Transition in Covalently Bonded DA Systems

One of the targets of this D/A system is to find materials that exhibit the N–I transition driven by a perturbation of external parameters such as temperature, pressure, and photoirradiation. Organic DA systems are the pioneers for such N–I transition materials,[35] and the best-known material is a tetrathiafulvalene/*p*-chloranil compound (TTF-CA) discovered by Torrance and co-workers in 1981.[24,36] Because organic N–I transition materials have been found in the vicinity of the valley of Torrance's V-shaped diagram,[24] the neutral D/A combinations located at around $\Delta E_{1/2}$(DA) ≈ 400 mV (i.e., the Madelung potential) in Figure 5 possibly exhibit the N–I transition. In fact, the DA chain compound, [Ru_2(2,3,5,6-F_4PhCO_2)$_4$(DMDCNQI)]·2(*p*-xylene) (2,3,5,6-$F_4PhCO_2^-$ = 2,3,5,6-tetrafluorobenzoate), which exhibited a temperature-induced N–I transition, was obtained (purple triangle in Figure 5).[27]

The N–I transition in this system can be definitely identified from the structural change, in addition to the variation of spin correlation. In particular, the structural change is sensitive to the charge on the respective units of D and A. This definition method to determine the charge distribution is useful for all of our systems independent of the type of A, either $TCNQR_x$ or $DCNQIR_x$. For the D unit, the Ru–O_{eq} length (O_{eq} = equatorial carboxylate oxygen atoms, see the inset of Figure 8a) is quite sensitive to the oxidation state of the [Ru_2] unit: 2.06–2.07 Å for [$Ru_2^{II,II}$] and 2.02–2.03 Å

for $[Ru_2^{II,III}]^+$.[9] This is quite reasonable, because two δ-type frontier orbitals are used for Ru−O_{eq} and Ru−Ru bondings, respectively, so the redox associated with the electron in the δ^* frontier orbital that makes the Ru−Ru bond (see Figure 2a) also strongly affects the Ru−O_{eq} bond (the variation of Ru−O_{eq} bonds is more characteristic than that of the Ru−Ru bond strongly affected by the axial ligand). Figure 8a shows the variation of the average Ru−O_{eq} bond length as a function of temperature.[27] There is a two-step variation with phase transition temperatures, T_1 and T_2 ($T_1 > T_2$). Following the aforementioned rule, the oxidation state of $[Ru_2]$ is $[Ru_2^{II,II}]$ at $T > T_1$ and $[Ru_2^{II,III}]^+$ at $T < T_2$. In between T_1 and T_2, the oxidation state is between both oxidation states, namely $[Ru_2]^{\delta+}$ where δ is formally ≈0.5 (intermediate phase, IM phase).

For the A unit, we can see the clear distinction between the quinonoid structure for the N state and quasi-benzenoid structure for the I state (Figure 8d). Neutral DMDCNQI has a quinonoid structure with characteristic single (*b* and *d* in Figure 8d), double (C=C; *c* and *e*), and triple (C≡N; *a*) bonds, whereas anionic DMDCNQI (i.e., $DMDCNQI^{\bullet-}$) has a nearly benzenoid structure with an unpaired electron delocalized over the entire complex, causing an averaging of the bond lengths. In the process of changing from N to I, the multiple bonds of *a*, *c*, and *e* should become longer, whereas the single bonds of *b* and *d* became shorter. Meanwhile, bond *f*, which is not involved in the resonance scheme, could not be affected by this alternation. In fact, as shown in Figure 8b, these variations occur at T_1 (ca. 270 K) and T_2 (ca. 210 K) in a stepwise manner upon cooling.[27]

Thus, the charge δ on $TCNQR_x^{\delta-}$ or $DCNQIR_x^{\delta-}$ can be roughly estimated from the structure using the Kistenmacher relationship[37] $\delta = -\{A[c/(b + d)] + B\}$, where the constants *A* and *B* are decided by assuming a completely neutral and a fully $1e^-$ ionized form of $TCNQR_x$/$DCNQIR_x$. For example, taking $TCNQ^0$ [38] and RbTCNQ[39] as standard compounds for δ = 0 and 1, respectively, $A_{TCNQ} = -41.667$ and $B_{TCNQ} = 19.833$ are obtained using the structural data reported previously, which are available for the $TCNQR_x$ series, and taking $[Rh_2^{II,II}(CF_3CO_2)_4$-(DMDCNQI)] ($\delta = 0$)[19] and $[Mn^{III}$(TMesP)(DMDCNQI)] (TMesP = *meso*-tetrakis(2,4,6-trimethylphenyl)porphyrinate; $\delta = 1$),[40] they are $A_{DCNQI} = -36.900$ and $B_{DCNQI} = 17.295$, also available for the $DCNQIR_x$ series. Figure 8c shows a plot of the estimated δ values for this N−I transition compound using the latter constants, and we confirm a two-step variation between N and I phases at T_1 and T_2 ($T > T_1$, N phase; $T_1 > T > T_2$, IM phase; $T < T_2$, I phase), consistent with the features of the $[Ru_2]$ unit (Figure 8a).[27]

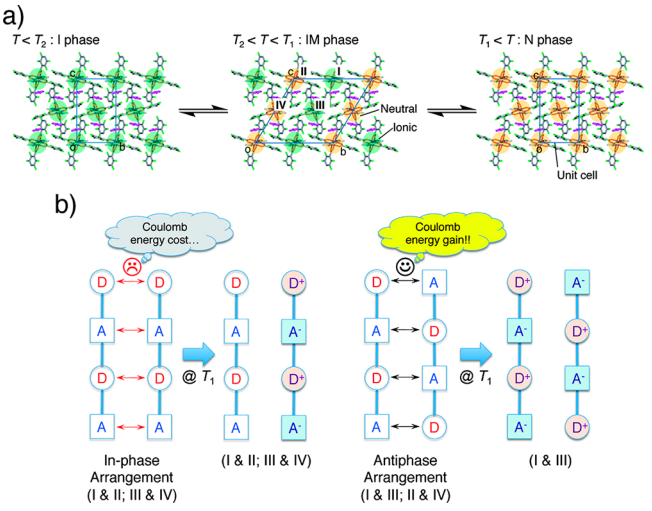

FIGURE 9. Packing arrangements of N and I chains in the N phase above T_1 (right), IM phase between T_1 and T_2 (center), and I phase below T_2 (left) (a), where the N and I phases crystallize in the monoclinic space group $P2_1/n$ and the IM phase crystallizes in the triclinic space group *P*-1 having four structurally independent chains of neutral II and IV and ionic I and III.[27] Schematic representation of arrangements of N and I chains at the first N−I transition at T_1 (b).

This is the first example of an N−I transition in a covalently bonded D/A system, and the CT between D^0A^0 and D^+A^- can be well explained by the affinity of D and A, as proved by the ionicity diagram in Figure 5. Here, the biggest interest is this: what is the IM phase with a formal δ of ≈0.5. The answer is simple, but a matter of vital importance: it is a mixture resulting from a homogeneous distribution of N and I chains (i.e., 50/50%) self-organized by responding to Coulombic interactions among adjacent chains (Figure 9).[27] A Coulomb energy cost is necessary for two chains aligned in-phase to change simultaneously from N to I states, whereas chains aligned antiphase have a Coulomb energy gain to become I chains (Figure 9b). Below T_2, the intrachain energy gain of the I state becomes large enough to overcome the Coulomb energy cost, allowing a uniform I state to form. This result is an experimental verification for the predictions of 30 years ago.[41−43] The most important aspect is the fact that Coulomb interactions, as well as the relation between I_D of D and E_A of A used, control the long-range charge distribution in the solid state of homogeneous species.

Summary and Outlook

In this Account, I have described our recent work on the rational design of D/A-MOFs and the control of CT in the frameworks. Our purpose in this work is rationally to design electronic/magnetic functional materials, in which both the

local spins and hopping electrons synergistically interact. I have not made particular reference to electronic properties, such as electron transport properties, of materials in this paper, but the present D/A materials often provide interesting electronic conducting properties closely associated with CT states.[22,27,34,44] As aforementioned, the CT materials based on transition metal complexes (i.e., D/A-MOFs) are literally a "reservoir of functions", in which we can treat both the localized static spins and hopping and/or itinerant electrons in the same system via "controllable charge transfer". In addition, the high redox activity of D/A-MOFs provides the high potential field in coordination space needed for the activation of inserted guest molecules; namely, it should be possible to create a unique system exhibiting lattice−guest interactions. Such a system conjures up an image of multifunctional molecular systems where chemical reactions in pore and physical phenomena on lattices are synergistically invoked.

The author gratefully acknowledges the contributions of his coworkers and collaborators whose names are listed in the papers produced by his group. The author is thankful for financial support from a Grant-in-Aid for Scientific Research from the Ministry of Education, Culture, Sports, Science, and Technology, Japan, The Sumitomo Foundation, and The Asahi Glass Foundation.

BIOGRAPHICAL INFORMATION

Hitoshi Miyasaka received his Ph.D. (1997) from Kyushu University under the supervision of Prof. H. Okawa and Prof. N. Matsumoto. Then, he joined the group of Prof. S. Kitagawa at Kyoto University as a postdoctoral researcher of JSPS (1998−2000). During one year from the end of 1999, he was a postdoctoral researcher in the group of Prof. K. R. Dunbar at Texas A&M University. In October 2000, he became an assistant professor at Tokyo Metropolitan University. He was also a research member of the PRESTO project of JST in 2002−2004. In 2006, he became an associate professor at Tohoku University in Sendai. Since April in 2011, he has been a professor at Kanazawa University. He received the Chemical Society of Japan Award for Young Chemists for 2003 and the Young Researcher Award of the Minister of Education, Culture, Sports, Science, and Technology for 2006. His current research interests are functional molecular materials involved in unique electronic/magnetic/chemical reaction systems.

FOOTNOTES

*Tel: +81-76-264-5697. Fax: +81-76-264-5742. E-mail: miyasaka@se.kanazawa-u.ac.jp.
The author declares no competing financial interest.

REFERENCES

1 Coronado, E.; Galán-Mascarós, J. R. Hybrid molecular conductors. *J. Mater. Chem.* **2005**, *15*, 66–74.

2 Coronado, E.; Day, P. Magnetic Molecular Conductors. *Chem. Rev.* **2004**, *104*, 5419–5448.

3 Enoki, T.; Akira, M. Magnetic TTF-Based Charge-Transfer Complexes. *Chem. Rev.* **2004**, *104*, 5449–5477.

4 Saito, G.; Yoshida, Y. Development of Conductive Organic Molecular Assemblies: Organic Metals, Superconductors, and Exotic Functional Materials. *Bull. Chem. Soc. Jpn.* **2007**, *80*, 1–137.

5 Miller, J. S.; Epstein, A. J. Organic and Organometallic Molecular Magnetic Materials—Designer Magnets. *Angew. Chem., Int. Ed. Engl.* **1994**, *33*, 385–415.

6 Creutz, C.; Taube, H. Binuclear Complexes of Ruthenium Ammines. *J. Am. Chem. Soc.* **1973**, *95*, 1086–1094.

7 Demadis, K. D.; Hartshorn, C. M.; Meyer, T. J. The Localized-to-Delocalized Transition in Mixed-Valence Chemistry. *Chem. Rev.* **2001**, *101*, 2655–2685.

8 Kitagawa, S.; Kitaura, R.; Noro, S. Functional Porous Coordination Polymers. *Angew. Chem., Int. Ed.* **2004**, *43*, 2334–2375.

9 Cotton, F. A.; Walton, R. A. *Multiple Bonds Between Metal Atoms*, 2nd ed.; Oxford University Press: Oxford, England, 1993.

10 Mehrotra, R. C.; Bohra, R. *Metal Carboxylates*; Academic Press: London, England, 1983.

11 Aquino, M. A. S. Diruthenium and Diosmium Tetracarboxylates: Synthesis, Physical Properties and Applications. *Coord. Chem. Rev.* **1998**, *170*, 141–202.

12 Miyasaka, H.; Clérac, R.; Campos-Fernández, C. S.; Dunbar, K. R. The First Crystal Structure of a One-Dimensional Chain of Linked Ru^{II}═Ru^{II} Units. *J. Chem. Soc., Dalton Trans.* **2001**, 858–861.

13 Furukawa, S.; Ohba, M.; Kitagawa, S. Rational Synthesis of a Two-Dimensional Honeycomb Structure Based on a Paramagnetic Paddlewheel Diruthenium Complex. *Chem. Commun.* **2005**, 865–867.

14 Mikuriya, M.; Yoshioka, D.; Handa, M. Magnetic Interactions in One-, Two-, and Three-Dimensional Assemblies of Dinuclear Ruthenium Carboxylates. *Coord. Chem. Rev.* **2006**, *250*, 2194–2211.

15 Miyasaka, H.; Motokawa, N.; Atsuumi, R.; Kamo, H.; Asai, Y.; Yamashita, M. Tuning of the Ionization Potential of Paddlewheel Diruthenium(II,II) Complexes with Fluorine Atoms on the Benzoate Ligands. *Dalton Trans.* **2011**, *40*, 673–682.

16 Kaim, W.; Moscherosch, M. The Coordination Chemistry of TCNE, TCNQ and Related Polynitrile π Acceptors. *Coord. Chem. Rev.* **1994**, *129*, 157–193.

17 Motokawa, N.; Oyama, T.; Matsunaga, S.; Miyasaka, H.; Sugimoto, K.; Yamashita, M.; Lopez, N.; Dunbar, K. R. A Ladder Based on Paddlewheel Diruthenium(II,II) Rails Connected by TCNQ Rungs: A Polymorph of the Hexagonal 2-D Network Phase. *Dalton Trans.* **2008**, 4099–4102.

18 Ouyang, X.; Campana, C.; Dunbar, K. R. A One-Dimensional Metallopolymer of 2,5-Dimethyl-N,N′-Dicyanoquinone Diimine (2,5-DM-DCNQI). *Inorg. Chem.* **1996**, *35*, 7188–7189.

19 Miyasaka, H.; Campos-Fernández, C. S.; Galán-Mascarós, J. R.; Dunbar, K. R. One-Dimensional Assemblies of Dirhodium Units Bridged by N,N′-Dicyanoquinodiimine Ligands. *Inorg. Chem.* **2000**, *39*, 5870–5873.

20 Miyasaka, H.; Campos-Fernández, C. S.; Clérac, R.; Dunbar, K. R. Hexagonal Layered Materials Composed of $[M_2(O_2CCF_3)_4]$ (M = Ru and Rh) Donors and TCNQ Acceptors. *Angew. Chem., Int. Ed.* **2000**, *39*, 3831–3835.

21 Miyasaka, H.; Izawa, T.; Takahashi, N.; Yamashita, M.; Dunbar, K. R. Long-Range Ordered Magnet of a Charge-Transfer Ru_2^{4+}/TCNQ Two-Dimensional Network Compound. *J. Am. Chem. Soc.* **2006**, *128*, 11358–11359.

22 Miyasaka, H.; Motokawa, N.; Matsunaga, S.; Yamashita, M.; Sugimoto, K.; Mori, T.; Dunbar, K. R. Control of Charge Transfer in a Series of $Ru_2^{II,II}$/TCNQ Two-Dimensional Networks by Tuning the Electron Affinity of TCNQ Units: A Route to Synergistic Magnetic/Conducting Materials. *J. Am. Chem. Soc.* **2010**, *132*, 1532–1544.

23 Nakabayashi, K.; Nishio, M.; Kubo, K.; Kosaka, W.; Miyasaka, H. An Ionicity Diagram for the Family of $[\{Ru_2(CF_3CO_2)_4\}_2(TCNQR_x)]$ ($TCNQR_x$ = R-Substituted 7,7,8,8-Tetracyano-p-quinodimethane). *Dalton Trans.* **2012**, *41*, 6072–6074.

24 Torrance, J. B.; Vazquez, J. E.; Mayerle, J. J.; Lee, V. Y. Discovery of a Neutral-to-Ionic Phase Transition in Organic Materials. *Phys. Rev. Lett.* **1981**, *46*, 253–257.

25 Lindsay, A. J.; Wilkinson, G. Reactions of Tetra-μ-carboxylato-diruthenium(II,II) Compounds. X-ray Crystal Structures of $Ru_2(\mu\text{-}O_2CCF_3)_4(thf)_2$, $Ru_2(\mu\text{-}O_2CR)_4(NO)_2$ (R = Et or CF_3), and $\{Na_3[Ru_2(\mu\text{-}O_2CO)_4]\cdot 6H_2O\}_n$. *J. Chem. Soc., Dalton Trans.* **1987**, 2723–2736.

26 McConnell, H. M.; Hoffman, B. M.; Metzger, R. M. Charge Transfer in Molecular Crystals. *Proc. Natl. Acad. Sci. U.S.A.* **1965**, *53*, 46–50.

27 Miyasaka, H.; Motokawa, N.; Chiyo, T.; Takemura, M.; Yamashita, M.; Sagayama, H.; Arima, T. Stepwise Neutral—Ionic Phase Transitions in a Covalently Bonded Donor/Acceptor Chain Compound. *J. Am. Chem. Soc.* **2011**, *133*, 5338–5345.

28 Cogne, A.; Belorizky, E.; Laugier, J.; Rey, P. Nitroxide Complexes of Diruthenium(II,II) Carboxylates. Structural and Magnetic Properties. *Inorg. Chem.* **1994**, *33*, 3364–3369.

29 Miyasaka, H.; Clérac, R.; Campos-Fernández, C. S.; Dunbar, K. R. Metal—Metal Bonded Diruthenium(II,III) Assemblies with the Polycyano Anionic Linkers $N(CN)_2^-$, $C(CN)_3^-$, and 1,4-Dicyanamido-2,5-dimethylbenzene ($DM\text{-}Dicyd^{2-}$): Syntheses, Structures, and Magnetic Properties. *Inorg. Chem.* **2001**, *40*, 1663–1671.

30 Motokawa, N.; Oyama, T.; Matsunaga, S.; Miyasaka, H.; Yamashita, M.; Dunbar, K. R. Charge-Transfer Two-Dimensional Layers Constructed from a 2:1 Assembly of

Paddlewheel Diruthenium(II,II) Complexes and Bis[1,2,5]thiadizolotetracyanoquinodimethane: Bulk Magnetic Behavior as a Function of Inter-Layer Interactions. *CrystEngComm* **2009**, *11*, 2121–2130.

31 Motokawa, N.; Matsunaga, S.; Takaishi, S.; Miyasaka, H.; Yamashita, M.; Dunbar, K. R. Reversible Magnetism between an Antiferromagnet and a Ferromagnet Related to Solvation/Desolvation in a Robust Layered $[Ru_2]_2$TCNQ Charge-Transfer System. *J. Am. Chem. Soc.* **2010**, *132*, 11943–11951.

32 Motokawa, N.; Miyasaka, H.; Yamashita, M.; Dunbar, K. R. An Electron-Transferred Ferromagnet with $T_c = 107$ K Based on a Three-Dimensional $[Ru_2]_2$/TCNQ System. *Angew. Chem., Int. Ed.* **2008**, *47*, 7760–7763.

33 Motokawa, N.; Miyasaka, H.; Yamashita, M. Pressure Effect on the Three-Dimensional Charge-Transfer Ferromagnet $[\{Ru_2(m\text{-}FPhCO_2)_4\}_2(BTDA\text{-}TCNQ)]$. *Dalton Trans.* **2010**, *39*, 4724–4726.

34 Miyasaka, H.; Morita, T.; Yamashita, M. A Three-Dimensional Network of Two-Electron-Transferred $[Ru_2]_2$TCNQ Exhibiting Anomalous Conductance due to Charge Fluctuations. *Chem. Commun.* **2011**, *47*, 271–273.

35 Horiuchi, S.; Kumai, R.; Okimoto, Y.; Tokura, Y. Chemical Approach to Neutral−Ionic Valence Instability, Quantum Phase Transition, and Relaxor Ferroelectricity in Organic Charge-Transfer Complexes. *Chem. Phys.* **2006**, *325*, 78–91.

36 Torrance, J. B.; Girland, A.; Mayerle, J. J.; Crowley, J. I.; Lee, V. Y.; Batail, P. Anomalous Nature of Neutral-to-Ionic Phase Transition in Tetrathiafulvalene-Chloranil. *Phys. Rev. Lett.* **1981**, *47*, 1747–1750.

37 Kistenmacher, T. J.; Emge, T. J.; Bloch, A. N.; Cowan, D. O. Structure of the Red, Semiconducting Form of 4,4′,5,5′-Tetramethyl-$\Delta^{2,2'}$-bi-1,3-diselenole-7,7,8,8-tetracyano-p-quinodimethane, TMTSF-TCNQ. *Acta Crystallogr., Sect. B* **1982**, *38*, 1193–1199.

38 Long, R. E.; Sparks, R. A.; Trueblood, K. N. The Crystal and Molecular Structure of 7,7,8,8-Tetracyanoquinodimethane. *Acta Crystallogr.* **1965**, *18*, 932–939.

39 Hoekstra, A.; Spoelder, T.; Vos, A. The Crystal Structure of Rubidium 7,7,8,8-Tetracyanoquinodimethane, Rb-TCNQ, at −160 °C. *Acta Crystallogr., Sect. B* **1972**, *28*, 14–25.

40 Sugiura, K.; Mikami, S.; Johnson, M. T.; Raebiger, J. W.; Miller, J. S.; Iwasaki, K.; Okada, Y.; Hino, S.; Sakata, Y. Ferrimagnetic Ordering of One-Dimensional N,N′-Dicyanoquinone Diimine (DCNQI) Electron Transfer Salts with Porphyrinatomanganese(II). *J. Mater. Chem.* **2001**, *11*, 2152–2158.

41 Hubbard, J.; Torrance, J. B. Model of the Neutral−Ionic Phase Transition. *Phys. Rev. Lett.* **1981**, *47*, 1750–1754.

42 Bak, P. Commensurate Phases, Incommensurate Phases and the Devil's Staircase. *Rep. Prog. Phys.* **1982**, *45*, 587–629.

43 Bruinsma, R.; Bak, P.; Torrance, J. B. Neutral−Ionic Transitions in Organic Mixed-Stack Compounds. *Phys. Rev. B* **1983**, *27*, 456–466.

44 Miyasaka, H.; Asai, Y.; Motokawa, N.; Kubo, K.; Yamashita, M. Magnetic/Conducting Bifunctionality due to π/σ-Conjugated Functional Moieties in a Stacked Ferrimagnetic Chain. *Inorg. Chem.* **2010**, *49*, 9116–9118.